Available online at www.sciencedirect.com
SCIENCE DIRECT®

Journal of the European Ceramic Society 24 (2004) 1489–1492

www.elsevier.com/locate/jeurceramsoc

Copper-doped hexagonal barium titanate ceramics

H.T. Langhammer[a,*], T. Müller[b], R. Böttcher[c], V. Mueller[a], H.-P. Abicht[b]

[a]*Fachbereich Physik, Martin-Luther-Universität Halle-Wittenberg, Friedemann-Bach-Pl. 6, D-06108 Halle, Germany*
[b]*Fachbereich Chemie, Martin-Luther-Universität Halle-Wittenberg, Kurt-Mothes-Str. 2, D-06120 Halle, Germany*
[c]*Fakultät für Physik und Geowissenschaften, Universität Leipzig, Linnéstraße 5, D-04103 Leipzig, Germany*

Abstract

The crystallographic phase, microstructure and dielectric properties of $BaTiO_3 + 0.02\ BaO + x\ CuO$ ceramics are studied at various Cu-doping level ($0 \leqslant x \leqslant 0.02$). It is confirmed by electron paramagnetic resonance that Cu_{Ti}^{2+} occupies Ti lattice-sites. Tetragonal and hexagonal phase coexist at room temperature for $x \geqslant 0.003$ (air-sintered, 1400 °C). The portion of tetragonal phase decreases with x, leading to a decrease and broadening of the dielectric anomaly at the Curie temperature. Although, as compared to other 3d transition dopants (e.g., Mn), the hexagonal phase is stabilized at room temperature at smaller Cu-concentration, the tetragonal phase does not vanish completely even at higher doping level. Grains with exaggerated, plate-like shape (mean grain size >100 μm) are attributed to the hexagonal phase. We suggest that Jahn-Teller distortion due to the d^9 electron configuration of Cu_{Ti}^{2+} represents the driving force for the cubic–hexagonal phase transition.

Keywords: $BaTiO_3$ and titanates; Cu-doped; Dielectric properties; Microstructure-final; X-ray methods

1. Introduction

Barium titanate ceramics represent a material system of fundamental importance for a wide range of technical applications. Although there were, depending on temperature, five different phases observed, the focus of research was on the cubic and tetragonal phase, respectively, which transform into each other at the paraelectric–ferroelectric phase transition temperature near 125 °C. Much less information is available about the hexagonal high temperature phase, which is stable at temperatures >1430 °C[1] as far as undoped, air-sintered material is concerned. The stability range of the hexagonal phase can be extended to room temperature both by firing in reducing atmospheres[2,3] and by doping with some acceptor-type 3d transition elements like Mn, Fe or Ni. [2,4]

Recently, Jahn-Teller distortion was proposed to be the common driving force for the cubic–hexagonal transition. Jahn-Teller distortion is caused by Ti_{Ti}^{3+} ions in the undoped material, or e.g., by Mn_{Ti}^{3+}.[4] To investigate this proposal, it appears to be useful to test also other Jahn-Teller active 3d transition elements. Like Mn_{Ti}^{3+}, also Cu_{Ti}^{2+} with its electron configurations d^9 exhibits a strong Jahn-Teller effect (JTE). However, to our knowledge, little is known about the occurrence of h-BT due to Cu-doping. Recently, we obtained first evidence that h-BT is produced by doping with 2 mol% Cu.[4,5]

Hence, the aim of this paper is the systematic investigation of the influence of Cu-doping on the crystallographic structure and macroscopic properties of $BaTiO_3$. To assist the desired Cu-incorporation on Ti-sites, a slight Ba-excess of the samples was maintained. X-ray diffraction (XRD) was used to investigate the global crystal structure of the specimens. Additional information was obtained by temperature-dependent dielectric measurements. Electron paramagnetic resonance (EPR) was applied for the investigation of the local structure of Cu_{Ti}^{2+} in the octahedral environment of oxygen. Since h-BT shows a particular bimodal grain growth behaviour,[3,4] the microstructural development of the samples was also in the focus of interest.

* Corresponding author. Tel.: +49-345-5525542; fax: +49-345-5527595.
E-mail address: langhammer@physik.uni-halle.de (H.T. Langhammer).

0955-2219/$ - see front matter © 2003 Elsevier Ltd. All rights reserved.
doi:10.1016/S0955-2219(03)00574-0

2. Experimental procedure

Ceramic powders with the nominal composition $BaTiO_3 + 0.02\ BaO + x\ CuO$ ($0 \leqslant x \leqslant 0.02$) were prepared by the conventional mixed-oxide powder technique.[4] Due to the thermodynamic instability of $BaTiO_3$ in water, the Ba:Ti ratio of the green bodies amounted to about 1.005 after fine-milling in water. The samples were sintered in air for 1 h at 1400 °C (heating rate 10 K/min). The microstructure of polished and chemically etched specimens was examined by optical microscopy and scanning electron microscopy (SEM). To determine the Cu-distribution in the grains and intergranular regions, wavelength-dispersive X-ray electron probe microanalysis (WDX-EPMA) (model CAMEBAX, Cameca, France) was carried out. The phase composition was determined quantitatively analyzing the XRD intensity ratios $(111)_{tetragonal}/(103)_{hexagonal}$ and $(200)_{tetragonal}/(103)_{hexagonal}$ (D5000 diffractometer, Siemens, Germany). Samples attached with silver electrodes were used to measure the complex small-signal permittivity. We analyze data obtained on cooling (cooling rate 0.7 K/min) and at the frequency 10 kHz. EPR measurements were carried out in the Q band (34.2 GHz) with a Bruker EMX device with 100 kHz field modulation. The magnetic field was determined by means of a proton magnetic-resonance probe. To avoid texture lines in the spectra, the samples were intensively crushed before.

3. Results and discussion

3.1. X-Ray diffraction and dielectric properties

The results of the XRD investigations are presented in Fig. 1. The percentage of tetragonal phase as a function of the Cu-doping level is shown. In the whole Cu-doping range investigated, exclusively tetragonal and hexagonal phases were found, within the detection limit of roughly 5 wt.%. Thus, the remaining percentage corresponds to the hexagonal phase. h-BT occurs above a minimum Cu-concentration of between 0.2 and 0.3 mol%. Its portion reaches a maximum value of about 90% around 1.5 mol% and is decreased again at 2.0 mol%.

The analysis of the dielectric measurements shows a qualitatively similar doping effect on ε'_{max} (permittivity maximum accompanying the paraelectric–ferroelectric phase transition, Fig. 1). This can easily be understood taking into account that the permittivity of the ceramic results from the superposition of the dielectric responses of ferroelectric (tetragonal) and non-ferroelectric (hexagonal) regions. Hence, the fact that ε'_{max} decreases with x reflects the decreasing volume of the (highly susceptible) tetragonal phase. In addition, we observe a broadening of the dielectric anomaly with increasing Cu-level whereas the phase transition temperature itself remains almost constant.

3.2. Microstructure and solubility of copper

The average grain sizes of the samples are shown in Fig. 2. Since the Ba-excess of the samples safely prevents the occurence of a Ti-rich liquid phase, the undoped or low-doped material exhibites normal grain growth with globular grains of 5–8 μm in diameter. For Cu-concentrations $x \geqslant 0.003$, the microstructure becomes bimodal. One fraction of grains remains globular with grain sizes only slightly increasing with x. The other fraction exhibits exaggerated grown, plate-like shaped grains with diameters $\geqslant 100$ μm. With increasing percentage of the plate-like fraction, these grains touch

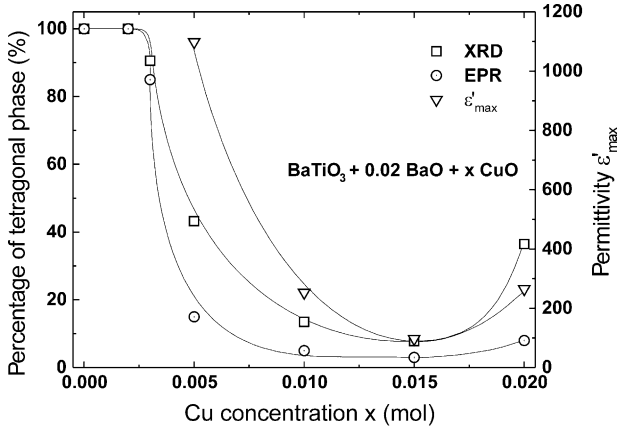

Fig. 1. Percentage of tetragonal phase at room temperature, as determined by XRD and EPR, plotted together with the maximum permittivity ε'_{max} at the Curie temperature as a function of the Cu content x.

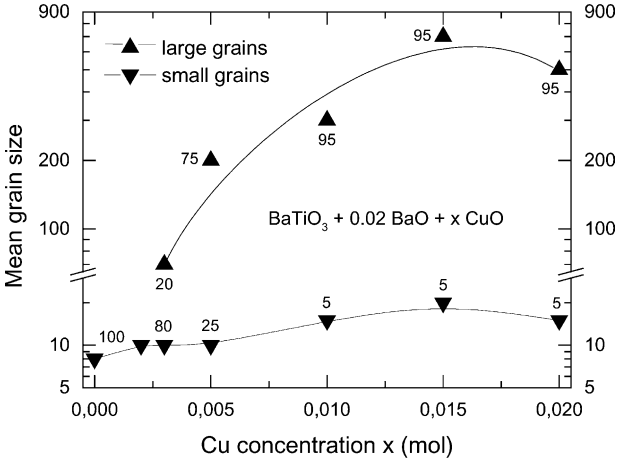

Fig. 2. Average grain size as a function of the nominal copper concentration. Numbers at data symbols denote the portions of grain fractions as we have it roughly estimated from the areas in a two-dimensional sample-cut.

each other during grain growth and the distinct plate-like shape vanishes gradually.

The Cu-distribution measured by EPMA is shown in Fig. 3 for the sample with $x = 0.02$. For all samples investigated, three different regions can be distinguished: the large, plate-like grains exhibit nearly the nominal doping concentration, whereas only 50% of the nominal value is incorporated into the small globular grains. Here the remaining dopant is segregated at the grain boundaries.

In view of the quite similar doping effect on the portion of hexagonal phase and on the fraction of exaggerated grains, it should be assumed that the plate-like, exaggerated grains belong to the hexagonal phase and the globular, small grain fraction to the tetragonal phase of $BaTiO_3$. Our results show that Cu-doping in $BaTiO_3$ leads to quite similar effects as doping with Mn, as far as the decreasing cubic–hexagonal phase transition temperature and the plate-like grain growth are concerned.[4] However, unlike to Mn-doped $BaTiO_3$, the small grains corresponding to tetragonal regions do not vanish completely with increasing doping level. This may be related to the lower solubility of Cu_{Ti}^{2+} in $BaTiO_3$, caused by its about 20% larger effective ionic radius (73 pm), as compared to the replaced Ti^{4+} (60.5 pm[6]).

3.3. Electron paramagnetic resonance

The first derivative of the absorption EPR spectra measured at room temperature shows two dominant quartets in the low-field range and intensive asymmetric lines in the field range of 11 800 G (Fig. 4, insert). Therefore, the data represent the superposition of two spectra corresponding to different surroundings of the Cu^{2+} ions in $BaTiO_3$. Each spectrum may be explained by an axial spin-Hamiltonian.[7] The $g_{\parallel}$ and $g_{\perp}$ components of the g tensor correspond to the quartet lines (hyper fine structure) and the intensive asymmetric lines, respectively. The analysis of the g values shows that both spectra can be attributed to $3d^9$ ions at distorted octahedral sites.[8,9] It is well known that the fivefold degenerated 3d orbitals are split by an octahedral crystal field into a triplet T_{2g} and a doublet E_g.[10] A tetragonal distortion, caused by the Jahn-Teller effect, e.g., splits the deeper lying electron state E_g of the $3d^9$ configuration further and an orbital-singlet ground state results. Consequently, the Cu^{2+} spectra measured in $BaTiO_3$ can be obtained only if the Cu^{2+} ions are in octahedral environments elongated along one of the cubic axes, leaving the ground state d_{x2-y2} orbitally non-degenerate. Since the Cu^{2+} ions are in octahedral environments and exhibit axial symmetry, it is very likely that they have occupied Ti-sites in the $BaTiO_3$ lattice, as it should also be expected from the effective ionic radii.

The intensity of both spectra depends crucially on the Cu-concentration. While increasing the Cu-concentration up to 1.5 mol%, the intensity of the lower-field quartet is decreased (Fig. 4). Since the doping effect on the EPR spectra corresponds nicely with the results of the XRD, dielectric and microstructural investigations, the spectra are attributed to Cu^{2+} impurities incorporated at two different tetragonally distorted CuO_6 octahedra, which reflect their tetragonal and hexagonal crystal

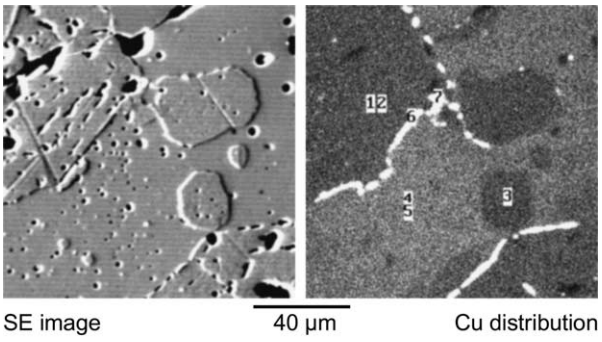

Fig. 3. SEM and EPMA images showing the copper distribution of a 2.0 mol% Cu-doped sample. The points indicated correspond to the copper concentrations: 0.96 (1), 1.06 (2), 0.92 (3), 2.11 (4), 2.13 (5) (values in mol%) and 19.5 (6), 10.5 (7) (values in wt.%).

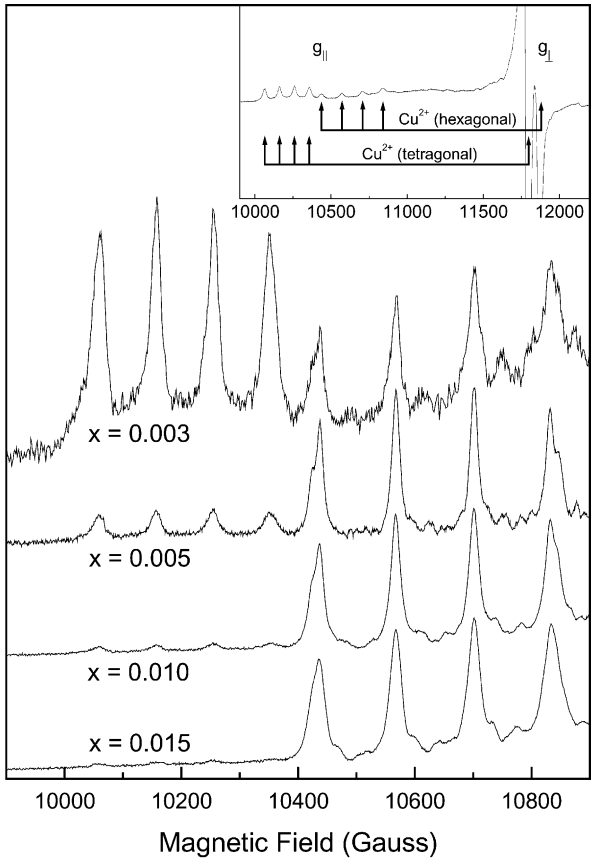

Fig. 4. Low-field part of the room-temperature EPR spectra for different copper concentrations x. The insert shows the whole spectrum ($g_{\parallel}$ and $g_{\perp}$) of a 2.0 mol% Cu-doped sample sintered at 1300 °C. Arrows indicate peaks with corresponding $g_{\parallel}$ and $g_{\perp}$ values.

surrounding, respectively. The intensity ratio between both Cu^{2+} spectra was used to calculate the percentage of Cu^{2+} ions with tetragonal surrounding. This is shown together with the XRD data in Fig. 1. Note that XRD-data reflect the global phase composition whereas EPR probes the local environment of the Cu^{2+} impurity. Hence, the EPR-data shown in Fig. 1 are systematically below the XRD-data. Nevertheless, both methods give the same threshold concentration for the occurrence of h-BT.

3.4. Doping effect on the cubic–hexagonal phase transformation

Two conditions are required for the high-temperature transformation of $BaTiO_3$ from its cubic into its hexagonal phase. First, a sufficiently high density of oxygen vacancies $V_O^{\circ\circ}$ is necessary to transform the Ba–O layers (the main constituents of the crystal structure of $BaTiO_3$) into the hexagonal stacking. Thus, as the oxygen vacancy density is increased due to charge compensation in acceptor(Cu_{Ti}^{2+})-doped $BaTiO_3$, the temperature of the minimum concentration [$V_O^{\circ\circ}$] decreases with the doping level. Second, a driving force should act as the initiator of the phase transformation. As in the case of Mn-doped and undoped $BaTiO_3$,[4] we prospose also for the Cu-doped material the influence of the Jahn-Teller distortion (see, e.g.[11]). The octahedral oxygen environment of Cu_{Ti}^{2+} with its d^9 configuration also causes a strong JTE. Hence, the resulting local lattice distortion may initiate the phase transition. Thus the lower transition temperature of the doped material can be explained. The phase transition takes place, provided that the concentrations both of the oxygen vacancies and of the JTE active acceptor ions are high enough and the ionic mobilities are sufficiently high. However, in the initial stage of the phase transition of a polycrystalline material, only few single crystallites (grains) transform which results in a phase coexistence in certain ranges of doping levels and sintering temperatures, respectively.

The differences between the effects of manganese and copper doping can be explained as follows. Whereas probably nearly all incorporated Cu exhibits the d^9 configuration, the JTE active Mn_{Ti}^{3+} (d^4) is the minority defect as compared to the dominating Mn_{Ti}^{4+} (d^3).[12] Therefore, at room temperature, $BaTiO_3$ doped with 0.5 mol% Mn is still completely tetragonal[4] while the same Cu-concentration causes a percentage of about 60% h-BT (in samples sintered at 1400 °C). However, in contrast to Mn-doped $BaTiO_3$ which is completely hexagonal for $[Mn_{Ti}] \geqslant 1.6$ mol%, Cu-doped material remains partially tetragonal. After a minimum of 8% is reached at 1.5 mol% Cu, the portion of tetragonal phase increases again at 2.0 mol%. The reason why the phase coexistence in Cu-doped $BaTiO_3$ is retained even at higher doping level is not clear yet.

4. Conclusions

Cu-doped $BaTiO_3$ ceramics sintered at 1400 C in air change gradually their room-temperature crystallographic structure from tetragonal to hexagonal, beginning with Cu-concentrations of between 0.2 and 0.3 mol%. EPR measurements revealed that Cu^{2+} is incorporated at two non-equivalent Ti-sites corresponding to different tetragonally distorted CuO_6 octahedra with tetragonal and hexagonal crystal surrounding, respectively. Contrary to Mn-doped $BaTiO_3$, for which also a decreased cubic–hexagonal phase transition temperature is observed, the hexagonal phase reaches a maximum percentage of 92% at 1.5 mol% Cu but does not replace the tetragonal phase completely. Basic results may be explained by the increasing stress in the hexagonal lattice caused by tetragonally distorted CuO_6 complexes. In addition, we suggest that the cubic-hexagonal phase transformation of Cu-doped $BaTiO_3$ is driven by Jahn-Teller distortion.

Acknowledgements

The authors thank Dr. Christian Eisenschmidt (Department of Physics, Martin-Luther-Universität Halle-Wittenberg) who carried out the XRD investigations.

References

1. Kirby, K. W. and Wechsler, B. A., Phase relations in the $BaTiO_3$–TiO_2 system. *J. Am. Ceram. Soc.*, 1991, **74**, 1841–1847.
2. Glaister, R. M. and Kay, H. F., An investigation of the cubic–hexagonal transition in barium titanate. *Proc. Phys. Soc.*, 1960, **76**, 763–771.
3. Kolar, D., Kunaver, U. and Rečnik, A., Exaggerated anisotropic grain growth in hexagonal barium titanate ceramics. *Phys. Stat. Sol (a)*, 1998, **166**, 219–230.
4. Langhammer, H. T., Müller, T., Felgner, K.-H. and Abicht, H.-P., Crystal structure and related properties of manganese-doped barium titanate ceramics. *J. Am. Ceram. Soc.*, 2000, **83**, 605–611.
5. Derling, S., Müller, T., Abicht, H.-P., Felgner, K.-H. and Langhammer, H. T., Copper oxide as a sintering agent for barium titanate based ceramics. *J. Mater. Sci.*, 2001, **36**, 1425–1431.
6. Shannon, R. D., Revised effective ionic radii and systematic studies of interatomic distances in halides and chalcogenides. *Acta Cryst. A*, 1976, **32**, 751–767.
7. Langhammer, H. T., Müller, T., Böttcher, R. and Abicht, H.-P., Crystal stucture and related properties of copper-doped barium titanate ceramics. *Solid State Sciences* (submitted).
8. Hathaway, B. J. and Billing, D. E., *Coordin. Chem. Rev.*, 1970, **5**, 143.
9. Warren, W. and Tuttle, B. A., *J. Am. Ceram. Soc.*, 1997, **80**, 860.
10. Abragam, A. and Bleany, B., *Electron Paramagnetic Resonance of Transition Ions*. Clarendon Press, Oxford, 1970.
11. Bersuker, I. B., The Jahn-Teller effect in crystal chemistry and spectroscopy. *Coord. Chem. Rev.*, 1975, **14**, 357–412.
12. Milsch, B., Evaluation of lattice site and valence of manganese in polycrystalline $BaTiO_3$ and n-$BaTiO_3$ by electron paramagnetic resonance. *Phys. Stat. Sol. (a)*, 1992, **133**, 455–464.